Semiconductors, Vol. 39, No. 3, 2005, pp. 336–342. Translated from Fizika i Tekhnika Poluprovodnikov, Vol. 39, No. 3, 2005, pp. 354–360.

SEMICONDUCTOR STRUCTURES, INTERFACES, AND SURFACES

Vegard's Law and Superstructural Phases in $Al_xGa_{1-x}As$/GaAs(100) Epitaxial Heterostructures

É. P. Domashevskaya*^, P. V. Seredin*, É. A. Dolgopolova*, I. E. Zanin*, I. N. Arsent'ev, D. A. Vinokurov**^^, A. L. Stankevich**, and I. S. Tarasov****

**Voronezh State University, Universitetskaya pl. 1, Voronezh, 394006 Russia*

^e-mail: root@ftt.vsu.ru

***Ioffe Physicotechnical Institute, Russian Academy of Sciences, Politekhnicheskaya ul. 26, St. Petersburg, 194021 Russia*

^^e-mail: dmitry.vinokurov@mail.ioffe.ru

Submitted May 25, 2004; accepted for publication June 7, 2004

Abstract—The lattice constants of $Al_xGa_{1-x}As$ epitaxial alloys with various AlAs (x) contents are determined for $Al_xGa_{1-x}As$/GaAs(100) heterostructures grown by MOC-hydride epitaxy using X-ray diffractometry and an X-ray back-reflection method. An ordered $AlGaAs_2$ (superstructural) phase is found in epitaxial heterostructures with $x \approx 0.50$. The lattice constant of this phase is smaller than the lattice constants of an $Al_{0.50}Ga_{0.50}As$ alloy and GaAs single-crystal substrate. © *2005 Pleiades Publishing, Inc.*

1. INTRODUCTION

The main tendency in the development of modern electronics is the use of submicron- and nanometer-sized functional objects (components). The unique properties of these objects (nanostructures) are determined by the atomic and electron processes both in the bulk and at the boundaries of heterostructures [1]. In this context, researchers are currently intensively developing both the theory of the phenomena in small objects, the so-called low-dimensional systems, and new precision methods for their study [2]. It is well known that isomorphic compounds, including AlAs and GaAs, form continuous solid solutions [3]. For epitaxial growth, the lattice matching of a film and a substrate possessing different chemical compositions is of great importance. The $Al_xGa_{1-x}As$/GaAs heterostructure possesses this property. This structure, whose lattice mismatch is $\lesssim 0.15\%$, is widely used in various structures and devices [4].

Gallium arsenide is the best-studied and most widely used III–V material. In contrast, AlAs is one of the least known compounds, which can be explained by its very high melting point (1700°C) and its instability, which is due to its decomposition in air. Gallium arsenide and AlAs both have sphalerite crystal lattices with almost equal values for the lattice constants and ionicity; as a result, the growth of $Al_xGa_{1-x}As$ layers on GaAs substrates is quite straightforward and the crystal quality of the obtained alloys is relatively high. A specific feature of this system is an increase in the crystal-lattice constants of the alloy in conjunction with an increase in the content of the Al atoms, which replace the Ga atoms in the metal sublattice, owing to the larger size of an Al atom.

When growing thin heteroepitaxial layers on a bulk substrate, the lattice mismatch, in some cases, does not cause the generation of misfit dislocations. However, the epitaxial layer is uniformly elastically strained in the plane parallel to the heterointerface [5]. Under these circumstances, in order to find the lattice constant of the alloy a^ν, taking into account the elastic strain in the heteroepitaxial layer, the normal and parallel components of the lattice constant, $a^\perp$ and $a^\parallel$, should be determined from the results of an X-ray diffraction analysis. According to the theory of elasticity, this constant can be calculated as [6]

$$a^\nu = a^\perp \frac{1-\nu}{1+\nu} + a^\parallel \frac{2\nu}{1+\nu}, \tag{1}$$

where ν are the Poisson ratios for the epitaxial layers.

The expressions for the lattice constants of the AlAs and AlGaAs epitaxial layers are written as [6]

$$a^\nu_{AlAs} = a^\perp_{AlAs} \frac{1-\nu_{AlAs}}{1+\nu_{AlAs}} + a^\nu_{GaAs} \frac{2\nu_{AlAs}}{1+\nu_{AlAs}}, \tag{2}$$

$$a^\nu_{Al_xGa_{1-x}As} = a^\perp_{Al_xGa_{1-x}As} \frac{1-\nu_{Al_xGa_{1-x}As}}{1+\nu_{Al_xGa_{1-x}As}} + a^\nu_{GaAs} \frac{2\nu_{Al_xGa_{1-x}As}}{1+\nu_{Al_xGa_{1-x}As}}, \tag{3}$$

where

$$\nu_{Al_xGa_{1-x}As} = x\nu_{AlAs} + (1-x)\nu_{GaAs},$$

1063-7826/05/3903-0336$26.00 © 2005 Pleiades Publishing, Inc.

and relation (3) can be rewritten as

$$a^{\nu}_{Al_xGa_{1-x}As} = a^{\perp}_{Al_xGa_{1-x}As}\frac{1-(x\nu_{AlAs}-(1-x)\nu_{GaAs})}{1+(x\nu_{AlAs}+(1-x)\nu_{GaAs})} + a^{\nu}_{GaAs}\frac{2(x\nu_{AlAs}+(1-x)\nu_{GaAs})}{1+(x\nu_{AlAs}+(1-x)\nu_{GaAs})}. \quad (4)$$

To calculate the lattice constants of the alloys, we used Poisson ratios taken from previously published data, namely $\nu_{AlAs} = 0.255$ [6, 7] and $\nu_{GaAs} = 0.312$ [8]. However, we experimentally determined only the $a^{\perp}$ components of the lattice constant for the heteroepitaxial structures, which correspond to measured values of the interplanar spacings $d^{\perp}$.

It is generally assumed that the dependence of the lattice constant on the Al content in the $Al_xGa_{1-x}As$ alloys follows Vegard's law [9]. However, the published data on the linearity or nonlinearity of the dependence of the lattice constants of alloys in the AlAs–GaAs system are contradictory [10, 11].

The purpose of this study is to determine the dependence of these lattice constants on the composition of $Al_xGa_{1-x}As$ epitaxial layers grown on a single-crystal GaAs (100) substrate by MOC-hydride epitaxy.

2. RESULTS AND DISCUSSION

2.1. Characteristics of the Epitaxial Structures under Study

The heterostructures under study were grown at the Ioffe Physicotechnical Institute. The epitaxial $Al_xGa_{1-x}As$ single-crystal films were grown on single-crystal GaAs (100) substrates by MOC-hydride epitaxy. The data on the Al content in the $Al_xGa_{1-x}As$ alloys and the film thicknesses are listed in Table 1.

Since the thickness of the $Al_xGa_{1-x}As$ films was rather large, it was possible to use an X-ray structure analysis to determine their lattice constants. The layer of half-absorptance for Cu$K\alpha_{1,2}$ radiation, which primarily diffracts the X-ray beam, was about 15 μm thick for the $Al_xGa_{1-x}As$/GaAs(100) system under study. Consequently, we could expect, at least for large angles, two independent reflections of different intensities, one from the film and the other from the substrate, which are caused by a lattice mismatch between the epitaxial film of the $Al_xGa_{1-x}As$ alloy and the GaAs (100) substrate. We determined the interplanar spacings and lattice constants of the $Al_xGa_{1-x}As$ epitaxial films and the GaAs (100) substrates for the samples under study using two methods of X-ray structure analysis, namely, X-ray diffractometry and, for the planar sample, the X-ray back-reflection method.

2.2. Results of Measurements of the Lattice Constants Using X-Ray Diffractometry

We carried out all the X-ray diffraction measurements using DRON-4-07 and DRON-3 diffractometers (Cu$K\alpha_{1,2}$ radiation). A specific feature of an X-ray diffraction analysis of single-crystal samples of a certain orientation is the fact that we can record very few X-ray diffraction lines; indeed, only one or two, but rarely three, are possible. The set of diffraction lines depends on the orientation of the single crystal during its growth. For example, for the $Al_xGa_{1-x}As$/GaAs(100) samples under study, there are only two diffraction lines, namely, the (200) line in the range from 31.10° to 31.80° and the (400) line in the range from 65.40° to 66.40°. Figure 1 shows the so-called full-range X-ray diffraction pattern of sample EM135, which was recorded over the entire angle range 2θ using the DRON-4-07 diffractometer. To determine the lattice constants of the epitaxial films, we selected the (400) line. The interplanar spacings and lattice constants at this stage of study were determined with an accuracy of ~0.001 Å.

When investigating the profiles of diffraction lines for multicomponent samples, the X-ray diffraction lines of various phases can overlap, which, in fact, occurs for $Al_xGa_{1-x}As$ films grown on a GaAs (100)

Table 1. Characteristics of the studied samples

Samples	Heterostructures	Thicknesses of epitaxial layers, μm
EM28	$Al_{0.12}Ga_{0.88}As$/GaAs	1
EM29	$Al_{0.16}Ga_{0.84}As$/GaAs	1
EM135	$Al_{0.50}Ga_{0.50}As$/GaAs	1
EM49	$Al_{0.54}Ga_{0.49}As$/GaAs	1
EM77	$Al_{>0.80}Ga_{<0.20}As/Al_{0.30}Ga_{0.70}As/Al_{>0.80}Ga_{<0.20}As$/GaAs	~0.5/0.2/0.1
EM72	AlAs/GaInP/AlAs/GaAs	~0.5/0.2/1

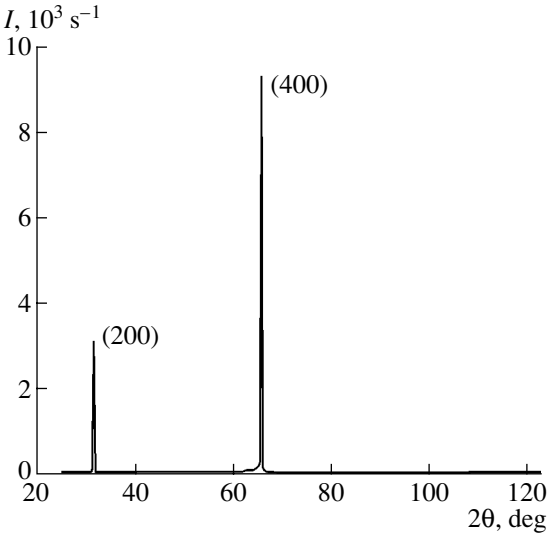

Fig. 1. The survey X-ray diffraction pattern of the $Al_{0.50}Ga_{0.50}As$/GaAs(100) epitaxial heterostructure.

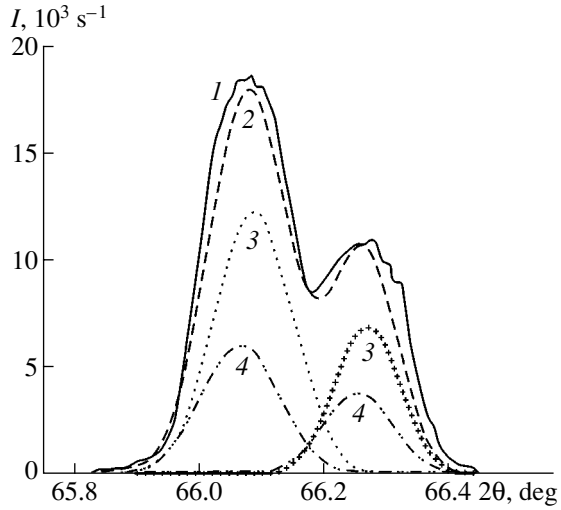

Fig. 2. Diffraction lines (400) from the $Al_{0.16}Ga_{0.84}As/GaAs(100)$ heterostructure. Curve *1* corresponds to the experiment, and curves *2–4* correspond to the approximation. The diffraction lines correspond to (*1*, *2*) the heterostructure, (*3*) GaAs (substrate), and (*4*) the $Al_{0.16}Ga_{0.84}As$ alloy.

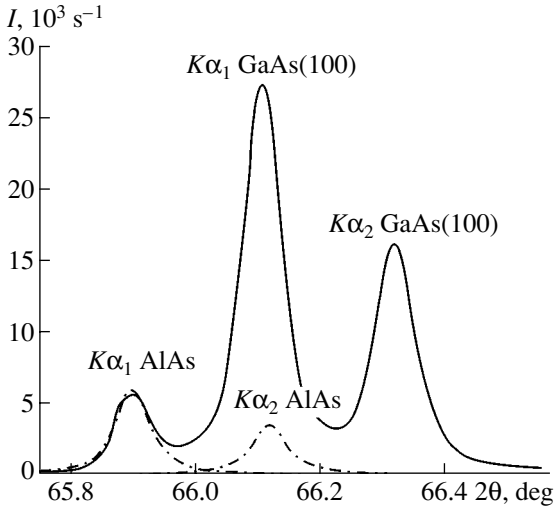

Fig. 3. Diffraction lines (400) for the AlAs/GaInP/AlAs/GaAs(100) heterostructure. The solid line corresponds to the experiment, and the dash-and-dot lines correspond to AlAs (approximation).

substrate. Since the atomic radii of Ga and Al do not significantly differ from each other, this overlap also occurs for the constants of the sphalerite lattices of GaAs and $Al_xGa_{1-x}As$ alloys.

Figure 2 shows the (400) diffraction line of the $Al_xGa_{1-x}As/GaAs$ heterostructure with a relatively low Al content ($x = 0.16$). It can be seen from this figure that the diffraction line of the $Al_xGa_{1-x}As$ epitaxial layer with low x practically merges with the diffraction line of the GaAs (100) substrate and appears as a single $K\alpha_{1,2}$ doublet with distorted lines. The shape of this doublet differs from the dispersion lines of the $K\alpha_{1,2}$ doublet for the single-crystal substrate due to the fact that the former doublet is the result of a superposition of two $K\alpha_{1,2}$ doublets. This circumstance introduces additional difficulties when attempting an exact determination of the lattice constants of epitaxial films. The results of the splitting of the (400) line into two $K\alpha_{1,2}$ doublets show (Table 2) that the alloy and the substrate are almost completely lattice-matched at low x. At the highest values of x (samples EM72 and EM77), the angular distance between the $K\alpha_{1,2}$ doublets of the film and the substrate is at its largest. Since the thickness of the film of the $Al_xGa_{1-x}As$ alloy is considerably larger than the thicknesses of the intermediate layers (GaInP in sample EM72 and $Al_{0.30}Ga_{0.70}As$ in sample EM77), the diffraction lines of the intermediate layers do not make much contribution to the (400) diffraction pattern. This circumstance allows us to calculate the lattice constants for these samples without resolving the lines into components (Fig. 3).

Table 2. Lattice constants of the $A_xGa_{1-x}As$ epitaxial films in the $Al_xGa_{1-x}As/GaAs(100)$ heterostructure

Sample no.	Value of x	Experiment		[11]
		$a^{\perp}$, Å	a^{v}, Å	a^{v}, Å
GaAs(100)	0	5.654	5.654	5.653
EM 28	0.12	5.655	5.655	5.654
EM 29	0.16	5.655	5.655	5.655
EM 135	0.50	5.661	5.658	5.657
EM 49	0.54	5.661	5.658	5.658
EM 77	>0.80	5.665	5.660	5.660
EM 72	1.00	5.667	5.661	5.661

Note: Values of $a^{\perp}$ are determined to within an accuracy of ±0.001 Å.

The solid line in Fig. 4 represents the (400) diffraction line of sample EM135, i.e., the $Al_{0.50}Ga_{0.50}As/GaAs(100)$ heterostructure. The profile of the (400) line for this sample includes five features in the form of peaks or so-called shoulders. It can be seen from the line profile that the diffraction line of the epitaxial film is superimposed onto the doublet from the substrate. To single out the diffraction line of the film, it is necessary to subtract the doublet of the (400) line of the GaAs (100) substrate from the integrated profile of the experimental line of the heterostructure. The reason for this subtraction is that the epitaxial film insignificantly weakens the Bragg reflection from the substrate by virtue of its small thickness ~1 μm [12].

After the subtraction of the experimental line corresponding to the $K\alpha_{1,2}$ doublet for the GaAs (100) substrate, three lines, lines (*1*), (*2*), and (*3*) (Fig. 4, curve *4*), remained instead of the expected single doublet from

the $Al_{0.50}Ga_{0.50}As$ alloy. Judging from the ratio of the intensities of the three remaining diffraction components for the epitaxial film, these lines are, in turn, the result of a superposition of two $K\alpha_{1,2}$ doublets. The first is the doublet from the alloy with $x = 0.50$ (lines (*1*) and (*2*)), which has a larger lattice constant than the substrate ($a^{\perp}_{x=0.5} > a^{\perp}_{GaAs}$). The second doublet is assigned to an unknown phase (un. ph.) in the same film, which has a smaller lattice constant than the substrate ($a^{\perp}_{un.ph} < a^{\perp}_{GaAs}$) (lines (*2*) and (*3*)). Using the Sigma Plot-8 software package to perform a regression analysis, we find that line (*2*) is indeed a superposition of two components: $K\alpha_2$, from the $Al_xGa_{1-x}As$ alloy with a larger $a^{\perp}$, and $K\alpha_1$, from the unknown phase in which $a^{\perp}$ is smaller than $a^{\perp}_{GaAs}$. The difference between the experimental (curve *1*) and simulated (curve *2*) profiles is about 10%. Thus, the studied profile of the (400) diffraction line of sample EM135 is the superposition of three $K\alpha_{1,2}$ doublets from different phases with almost equal lattice constants, namely, $a^{\perp}_{GaAs} = 5.654$ Å (substrate), $a^{\perp}_{x=0.50} = 5.661$ Å (film), and $a^{\perp}_{un.ph} = 5.646$ Å (film). Table 3 lists the results from the decomposition of the (400) line of the $Al_{0.50}Ga_{0.50}As/GaAs(100)$ heterostructure, specifically, the interplanar spacings $d^{\perp}$, lattice constant $a^{\perp}$, and lattice constant a^{ν} calculated using formula (4). A similar result was obtained by resolving the (400) line into components for sample EM49, where $x = 0.54$.

From the results of the decomposition into components, we determined the lattice constants of the $Al_xGa_{1-x}As$ alloys, which are given in Table 2 along with the lattice constants expected according to the linear Vegard's law given on the site of the Ioffe Physicotechnical Institute, Russian Academy of Sciences [11]. The lattice constants $a^{\perp}$ for the single-crystal GaAs (100) substrates, which are given in the first row of Table 2, have the same value both for all the studied heterostructures and for the GaAs (100) single-crystal wafer of corresponding thickness. Therefore, we used this value in formulas (2)–(4), assuming that $a^{\nu}_{GaAs} = a^{\perp}_{GaAs}$, in order to calculate a^{ν} for the AlAs and AlGaAs epitaxial films.

2.3. Results of Measurements of the Lattice Constants by the X-ray Back-Reflection Method

It has been shown in previous experiments with a KROS-1 camera that the X-ray photographic back-reflection method can be used at large diffraction angles to accurately measure the interplanar spacings and lattice constants of plane single-crystal samples. This measurement is achieved by rotating both the sample and the cassette with the X-ray film relative to the axis normal to the sample surface so that the planes with smallest interplanar spacings can occupy the reflecting position [12]. These planes cannot be recorded using a diffractometer because of the limitations of the goniometer.

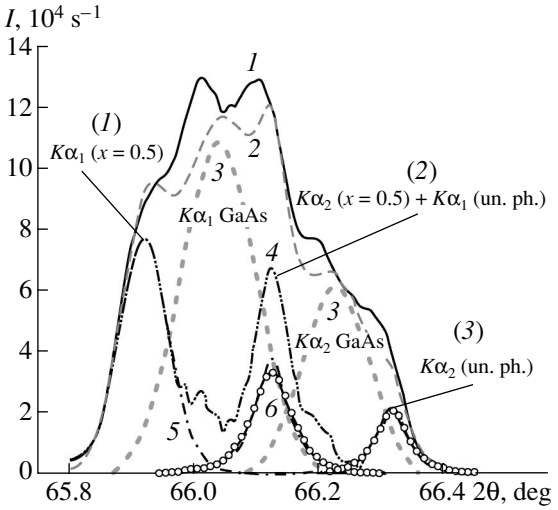

Fig. 4. Resolution of the (400) diffraction line of the $Al_{0.50}Ga_{0.50}As/GaAs(100)$ heterostructure. Curve *1* corresponds to the experiment, and curves *2*–*6* correspond to the approximation. The diffraction lines of (curves *1* and *2*) the heterostructure, (curve *3*) GaAs, (curve *4*) the heterostructure diffraction minus the diffraction from the substrate, (curve *5*) $Al_{0.5}Ga_{0.5}As$, and (curve *6*) an unknown phase (un. ph.) are shown; (*1*), (*2*), and (*3*) are the components of curve *4*.

In order to study samples EM28, EM29, EM49, and EM135, the camera was tuned to record the line (711) GaAs with the interplanar spacing $d = 0.7916$ Å [13]. The recording conditions were as follows: the anode voltage of the X-ray tube was 30 kV; the current, 15 mA; the distance between the sample and the cassette with film, 104 mm; the distance between the cassette and a diaphragm, 26.3 mm; and the exposure time, 1 h.

An analysis of the X-ray diffraction patterns obtained for samples EM28, EM29, and EM40 by the

Table 3. Results of resolving the (400) diffraction line of the $Al_{0.50}Ga_{0.50}As/GaAs(100)$ heterostructure (sample EM135)

Components of the heterostructure	$d^{\perp}$, Å	$I(K\alpha_2/K\alpha_1)$	$a^{\perp}_{expt}$, Å	a^{ν}, Å
GaAs(100) (substrate)	1.414	0.57	5.654	5.654
$Al_{0.50}Ga_{0.50}As$ (film)	1.415	0.54	5.661	5.658
An unknown Al–Ga–As phase (in the film)	1.412	0.54	5.646	5.650

Note: Values of d', $a^{\perp}$, and a^{ν} are determined to within an accuracy of ±0.001 Å; $a^{\perp}_{expt}$ are the experimental values.

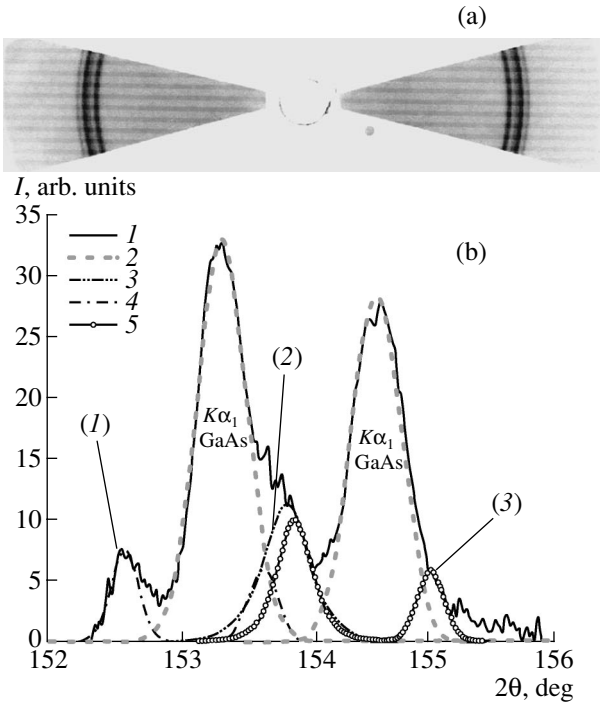

Fig. 5. (a) The Bragg reflection from the (711) planes of the $Al_{0.50}Ga_{0.50}As/GaAs(100)$ heterostructure recorded on X-ray film using the back-reflection method, and (b) the result of the digitization of this diffraction pattern. Curve *1* corresponds to the experiment, and the diffraction lines of (curve *2*) the GaAs substrate, (curve *4*) $Al_{0.5}Ga_{0.5}As$, and (curve *5*) an unknown phase (un. ph.) are shown. Curve *3* corresponds to the lines $K\alpha_2(x = 0.5) + K\alpha_1$(un. ph); (*1*), (*2*), and (*3*) represent the heterostructure diffraction minus the substrate diffraction.

back-reflection method using the KROS-1 camera without the rotation of the sample and the cassette with the X-ray film showed a slight deviation of the sample surface orientation from the (100) plane. Therefore, only the $K\alpha_2$ line of the GaAs (100) substrate in the X-ray diffraction patterns of these samples satisfied the conditions for the Bragg diffraction. As a result, it was impossible to obtain data on the crystal structure of the epitaxial films of these samples using the photographic method. However, we managed to obtain complete diffraction by the back-reflection method for sample EM135. Two doublets are present in the X-ray diffraction pattern obtained for this sample, namely, a more intense doublet from the GaAs (100) substrate and a doublet related to the $Al_{0.50}Ga_{0.50}As$ film (Fig. 5).

Table 4. Interplanar spacings and lattice constants determined from the (711) line for the $Al_{0.5}Ga_{0.5}As/GaAs(100)$ heterostructure

Sample no.	Components of the heterostructure	$a^{\perp}_{\text{expt}}$, Å	$a^{\perp}_{\text{expt}}$, Å	a^{ν}, Å	a^{ν}, Å [7]
EM 135	GaAs (substrate)	0.7916	5.6532	5.6532	5.6533
	$Al_{0.50}Ga_{0.50}As$ (film)	0.7927	5.6612	5.6582	5.6572
	An unknown phase (in the film)	0.7906	5.6465	5.6495	

Note: Values of $d^{\perp}$, $a^{\perp}$, and a^{ν} are determined to within an accuracy of 0.0001 Å.

The results of the diffraction onto the X-ray film at the (711) plane of this sample were processed using a procedure involving a digital representation of the data [12]. The result of this digitization is shown in Fig. 5. After resolving the (711) diffraction line into components, we obtained a result similar to the splitting of the (400) X-ray diffraction line for the same sample. Figure 5b shows that the (711) diffraction line is a superposition of three doublets. The first doublet is the most intense $K\alpha_{1,2}$ doublet for the substrate, the second doublet is the $K\alpha_{1,2}$ doublet for the $Al_{0.5}Ga_{0.5}As$ alloy with the interplanar spacing $d^{\perp}_{x=0.5} > d^{\perp}_{\text{GaAs}}$, and the third doublet is the doublet from the unknown phase (un. ph.) with the smaller interplanar spacing $d^{\perp}_{\text{un. ph}} < d^{\perp}_{\text{GaAs}}$. Table 4 lists the results from calculations of the interplanar spacings for the (711) planes and lattice constants.

3. DISCUSSION

According to the data obtained by the diffractometric and photographic methods of X-ray structure analysis, the lattice constant of the GaAs (100) substrate, for all the samples, practically coincides with the value given on the site of the Ioffe Physicotechnical Institute [11] when the experimental error is taken into account. The exact determination of the lattice constant for GaAs is of great importance, since this parameter is a reference point for further calculations, and the fact that the measured parameter remains constant for all the samples indicates that the reproducibility of the experimental results is high. The most accurate measurements of the lattice constant for GaAs (100) were obtained using the X-ray back-reflection method for the (711) line, and gave the value 5.6532 ± 0.0001 Å. This value coincides with that given in [11].

For Vegard's law in relation to the $Al_xGa_{1-x}As$ epitaxial layers, the lattice constant a^{ν} calculated taking into account the elastic stresses for alloys of various compositions depends linearly on the alloy composition in the AlAs–GaAs system given in [11] (see Fig. 6) for all the heterostructures (see Table 2). We also illustrated Vegard's law with line *1* in Fig. 6, which shows the quantities $a^{\perp}_{\text{expt}}$ determined from the experimentally measured $d^{\perp}_{\text{expt}}$.

In addition, the diffraction lines of an unknown phase with a lattice constant smaller than that of GaAs are found by resolving the (400) diffraction line for

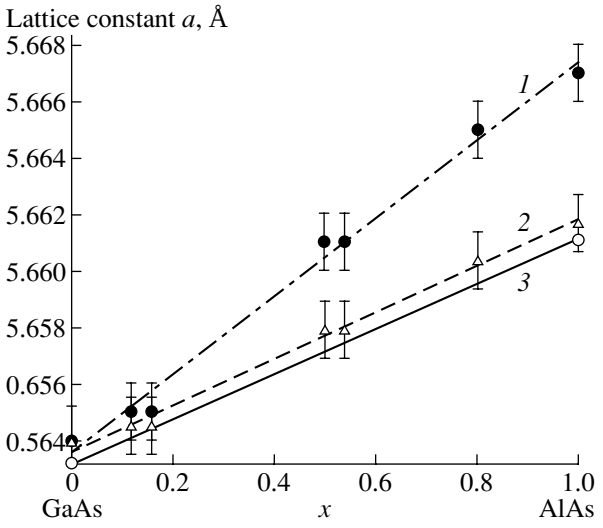

Fig. 6. Composition dependences of the lattice constants (Vegard's law) for the AlAs–GaAs system. Curve *1* corresponds to $a^{\perp}_{\text{expt}}$; curve *2*, to a^{v}; and curve *3*, to a^{v} [7].

samples EM49 and EM135. This is also the case for the (711) diffraction line for sample EM135.

The possible formation of superlattices in $Al_xGa_{1-x}As$ films at $x = 0.25$–0.75 has already been discussed in a number of publications [14–17]. Its formed ordered structure can have a tetragonal symmetry similar to the structure of an CuAu I alloy and consist of alternating AlAs and GaAs layers [14, 15]. However, an analysis of our results allows us to conclude that the unknown phase found during this investigation is an $AlGaAs_2$ chemical compound. This phase is a superstructure related to the sphalerite lattice, which is characteristic of GaAs, AlAs, and $Al_xGa_{1-x}As$ alloys. The lattice of the $AlGaAs_2$ phase that we identified can be described by a structure of the $InGaAs_2$ type (layered tetragonal) [18] with a [100] ordering direction. In this structure, the unit cell corresponds to the sphalerite-type cell doubled along the *c* axis. The ratio *c*/2*a*, observed in phases with this structure, can be both larger and smaller than unity [19].

The decrease in the lattice constant for the identified $AlGaAs_2$ superstructure is explained by the fact that the distribution of the Al and Ga atoms in the metal sublattice of an ideal $Al_xGa_{1-x}As$ alloy is statistical, and the lattice constant of the alloy is the average value of the lattice constants for the multitude of cells. In contrast, the $AlGaAs_2$ chemical compound is formed for a superstructure, and a so-called tetragonal compression of the layers filled with various Ga or Al atoms takes place. As a result, owing to the layered ordering of the sites of the Al and Ga atoms in the III sublattice, the lattice constant $c^{\perp} = 2a^{\perp}_{\text{AlGaAs}_2} = 11.292$ Å $< 2a^{\perp}_{x=0.5} = 11.322$ Å. In this case, the lattice constant $c^{\perp}$ is oriented along the normal to the (100) plane, i.e., the unit cell is tetragonally compressed in the growth direction of the epitaxial film, and the magnitude of this compression is $c^{\perp}_{\text{AlGaAs}_2}/2a^{\perp}_{x=0.5} = 0.997 < 1$ in the ordering region.

The ratio for the intensities of the $K\alpha_{1,2}$ doublets of the $AlGaAs_2$ superstructural phase and the alloy for the (400) and (711) reflections is indicative of the considerable volume (~15%) of regions in the $Al_{0.50}Ga_{0.50}As$ ordered alloy accompanied by the $AlGaAs_2$ superstructural phase in the epitaxial heterostructures in which $x \approx 0.50$.

4. CONCLUSIONS

Based on the studies carried out, we can put forward the following conclusions.

(i) Vegard's law is valid for $Al_xGa_{1-x}As$/GaAs(100) heterostructures grown by MOC-hydride epitaxy.

(ii) A superstructural phase is found in the Al_xGa_{1-x}AsGaAs (100) heterostructures with $x \approx 0.5$. This phase is an $AlGaAs_2$ chemical compound with the lattice constant $c^{\perp} = 2a^{\perp}_{\text{AlGaAs}_2} = 11.292$ Å. The magnitude of tetragonal distortion in the direction of the epitaxial growth is $a^{\perp}_{\text{AlGaAs}_2}/2a^{\perp}_{x=0.5} = 0.997$.

ACKNOWLEDGMENTS

We thank D.N. Nikolaev for his help during the experiments and V.V. Shamakhov for his valuable comments during a discussion of the results.

REFERENCES

1. Zh. I. Alferov, Fiz. Tekh. Poluprovodn. (St. Petersburg) **32**, 3 (1998) [Semiconductors **32**, 1 (1998)].
2. É. P. Domashevskaya, V. A. Terekhov, V. M. Kashkarov, *et al.*, Fiz. Tekh. Poluprovodn. (St. Petersburg) **37**, 1017 (2003) [Semiconductors **37**, 992 (2003)].
3. Zh. I. Alferov, V. M. Andreev, S. G. Konnikov, *et al.*, Krist. Tech. **11**, 1013 (1976).
4. *Molecular Beam Epitaxy and Heterostructures*, Ed. by L. L. Chang and K. Ploog (Martimus Nishoff, Amsterdam, 1985; Mir, Moscow, 1989).
5. I. N. Arsent'ev, N. A. Bert, S. G. Konnikov, and V. E. Umanskiĭ, Fiz. Tekh. Poluprovodn. (Leningrad) **14**, 96 (1980) [Sov. Phys. Semicond. **14**, 53 (1980)].
6. D. Zhou and B. F. Usher, J. Phys. D: Appl. Phys. **34**, 1461 (2001).
7. Z. R. Wasilewski, M. M. Dion, D. Lockwood, *et al.*, J. Appl. Phys. **81**, 1683 (1997).
8. S. Adachi, J. Appl. Phys. **58**, R1 (1985).
9. M. Herman, *Semiconductor Superlattices* (Akademie, Berlin, 1986; Mir, Moscow, 1989).

10. *Solid Solutions in Semiconductor Systems: A Handbook*, Ed. by V. S. Zemskov *et al.* (Nauka, Moscow, 1978) [in Russian].
11. *Characteristics of Semiconductor Materials* (Fiz.–Tekh. Inst., St. Petersburg), www.ioffe.ru.
12. P. V. Seredin, Kondens. Sredy Mezhfaz. Granitsy **5** (1) (2001).
13. *Diffraction Data Cards* (ASTM, 1972).
14. T. S. Kuan, T. F. Kuech, and W. I. Wang, Phys. Rev. Lett. **54**, 201 (1985).
15. B. Koiller and A. M. Davidovich, Phys. Rev. B **41**, 3670 (1990).
16. E. Muller, B. Patterson, *et al.*, PSI Annual Report 2000, www.physik.unizh.ch/reports/report2000.html.
17. B. D. Patterson *et al.*, PSI Annual Report 1997, www.physik.unizh.ch/reports/report1999.html.
18. Alex Zunger, MRS-IRS Bulletin (1997), http://www.sst.nrel.gov/images/mrs97.
19. W. B. Pearson, *Crystal Chemistry and Physics of Metals and Alloys* (Wiley, New York, 1972; Mir, Moscow, 1977), Parts 1, 2.

Translated by N. Korovin